Journal of Systems Engineering and Electronics
Vol. 32, No. 5, October 2021, pp.1014 – 1022

Event-triggered leader-following formation control for multi-agent systems under communication faults: application to a fleet of unmanned aerial vehicles

VAZQUEZ TREJO Juan Antonio[1,2,*], GUENARD Adrien[3], ADAM-MEDINA Manuel[2], PONSART Jean-Christophe[1], CIARLETTA Laurent[3], ROTONDO Damiano[4], and THEILLIOL Didier[1]

1. Research Center for Automatic Control of Nancy, University of Lorraine, Nancy F-54000, France;
2. Electronic Engineering Department, National Institute of Technology of Mexico, Cuernavaca Morelos 62490, Mexico;
3. Lorraine Research Laboratory in Computer Science and Its Applications, University of Lorraine, Nancy F-54000, France;
4. University of Stavanger, Department of Electrical and Computer Engineering, Stavanger 4021, Norway

Abstract: The main contribution of this paper is the design of an event-triggered formation control for leader-following consensus in second-order multi-agent systems (MASs) under communication faults. All the agents must follow the trajectories of a virtual leader despite communication faults considered as smooth time-varying delays dependent on the distance between the agents. Linear matrix inequalities (LMIs)-based conditions are obtained to synthesize a controller gain that guarantees stability of the synchronization error. Based on the closed-loop system, an event-triggered mechanism is designed to reduce the control law update and information exchange in order to reduce energy consumption. The proposed approach is implemented in a real platform of a fleet of unmanned aerial vehicles (UAVs) under communication faults. A comparison between a state-of-the-art technique and the proposed technique has been provided, demonstrating the performance improvement brought by the proposed approach.

Keywords: event-triggered, leader-following consensus, communication fault, formation control, unmanned aerial vehicle (UAV), experimental result.

DOI: 10.23919/JSEE.2021.000086

1. Introduction

Leader-following consensus for multi-agent systems (MASs) has attracted interest due to its applications in collective missions including, self-organization, clusters of satellites, formation flying, and sensor networks [1]. Leader-following consensus is a particular problem in multi-agent systems where all the agent trajectories must converge to the trajectory of a leader [2]. Several research works have increased the focus on considering multiplicative and additive noises [3], switching topologies [4], time delays [5], particle swarm optimization [6], and event-triggered mechanisms [7], among others. The information exchange through digital networks is a key point in leader-following consensus. However, delays [8], packet losses [9], communication faults [10], or bandwidth limitations [11] are challenges in real engineering applications [12].

An alternative control strategy is the event-triggered approach, which is often used for reducing the information exchange and the control law rate [13]. The difference between event-triggered and time-triggered approaches are that the latter considers a periodic control law update, whereas, in the former, the update of the control law and the information exchange between the agents are determined by an event generator [14,15]. Related works have increased the focus on event-triggered leader-following consensus in the last decades considering sufficient conditions using the M-matrix theory and algebraic inequalities for second-order nonlinear time-delayed dynamic agents [16]; linear matrix inequalities (LMIs)-based conditions using the M-matrix theory for reaching bipartite consensus in nonlinear second-order agents [17]; nonuniform delays in heterogeneous agents [8]; bounded delays in fractional-order agents [18]; sufficient conditions including dependent and independent fixed delays, and time-varying delays [19]; constant delays in linear agents [20]. Nevertheless, the aforementioned works have not considered a degradation in the communication based

Manuscript received December 24, 2020.
*Corresponding author.

on the distances between agents. In [10], communication faults are modeled as a modification in the weights of the adjacency matrix as a result of a malfunction in the exchange of information. The communication faults in this work are considered as a delay-dependent on the distances between agents. Unlike [21], where a time-triggered control is designed to tolerate smooth communication faults, the main contribution of this paper inspired by [7], is the design of an event-triggered strategy to solve the leader-following consensus problem in second-order MASs under communication faults. A synthesis of a robust control gain is obtained in order to tolerate faults in the exchange of information. Then, based on the closed-loop system, an event-triggered mechanism is used in order to reduce the information exchange between agents and the control update rate. The proposed technique has been implemented in a real platform comprising a fleet of unmanned aerial vehicles (UAVs) achieving a desired formation and following a virtual leader agent in spite of the degradation in the exchange of information.

This paper is organized as follows. Preliminaries and problem statement are provided in Section 2. The event-triggered leader-following formation control design is described in Section 3. The experimental results are shown in Section 4. Finally, the main conclusions are presented in Section 5.

2. Preliminaries and problem statement

2.1 Notation and graph theory

Given a matrix $\boldsymbol{X}$, $\boldsymbol{X}^{\mathrm{T}}$ denotes its transpose, $\boldsymbol{X}>0(<0)$ denotes a positive (negative) definite matrix. $\|\cdot\|$ denotes the Euclidean norm. For simplicity, the symbol $*$ within a symmetric matrix represents the symmetric entries. The Hermitian part of a square matrix $\boldsymbol{X}$ is denoted by $\mathbf{He}\{\boldsymbol{X}\}=\boldsymbol{X}+\boldsymbol{X}^{\mathrm{T}}$. The symbol $\otimes$ denotes the Kronecker product, which for real matrices $\boldsymbol{A}$,$\boldsymbol{B}$, $\boldsymbol{C}$, and $\boldsymbol{D}$ with appropriate dimensions, satisfing the following properties [22]:

(i) $(\boldsymbol{A}+\boldsymbol{B})\otimes\boldsymbol{C}=\boldsymbol{A}\otimes\boldsymbol{C}+\boldsymbol{B}\otimes\boldsymbol{C}$;

(ii) $(\boldsymbol{A}\otimes\boldsymbol{B})^{\mathrm{T}}=\boldsymbol{A}^{\mathrm{T}}\otimes\boldsymbol{B}^{\mathrm{T}}$;

(iii) $(\boldsymbol{A}\otimes\boldsymbol{B})(\boldsymbol{C}\otimes\boldsymbol{D})=(\boldsymbol{AC})\otimes(\boldsymbol{BD})$.

A directed graph $\mathcal{G}$ is a pair $(\mathcal{V},\mathcal{E})$, where $\mathcal{V}=\{\sqsubseteq_1,\cdots,\sqsubseteq_N\}$ is a non-empty finite node set (set of agents) and $\mathcal{E}=\{(i,j):i,j\in\mathcal{V}\}\subseteq\mathcal{V}\times\mathcal{V}$ is an edge set of ordered pairs of N nodes. The neighbors of the node i are denoted as $j\in\mathcal{N}_i$. The adjacency matrix $\mathcal{A}=[a_{ij}]\in\mathbb{R}^{N\times N}$ associated with the graph $\mathcal{G}$ is defined such that $a_{ii}=0$, $a_{ij}>0$ if and only if $(i,j)\in\mathcal{E}$ and $a_{ij}=0$ otherwise. The Laplacian matrix $\mathcal{L}=[\updownarrow_{ij}]\in\mathbb{R}^{N\times N}$ of the graph $\mathcal{G}$ is defined as $\updownarrow_{ii}=\sum_{j\neq i}a_{ij}$ and $\updownarrow_{ij}=-a_{ij}$, $i\neq j$.

Lemma 1 [23] For a given matrix $\begin{bmatrix}\boldsymbol{S}_1 & \boldsymbol{S}_2\\ \boldsymbol{S}_2 & \boldsymbol{S}_3\end{bmatrix}<0$, the following statements are equivalent:

(i) $\boldsymbol{S}_1<0$, $\boldsymbol{S}_3-\boldsymbol{S}_2^{\mathrm{T}}\boldsymbol{S}_1^{-1}\boldsymbol{S}_2<0$;

(ii) $\boldsymbol{S}_3<0$, $\boldsymbol{S}_1-\boldsymbol{S}_2^{\mathrm{T}}\boldsymbol{S}_3^{-1}\boldsymbol{S}_2<0$.

2.2 Problem statement

Consider the second-order MAS

$$\begin{cases}\dot{\boldsymbol{p}}_i(t)=\boldsymbol{v}_i(t)\\ \dot{\boldsymbol{v}}_i(t)=\boldsymbol{u}_i(t)\end{cases}\tag{1}$$

where $\boldsymbol{p}_i(t)$, $\boldsymbol{v}_i(t)$, $\boldsymbol{u}_i(t)\in\mathbb{R}^n$ are the position, velocity, and acceleration input with $\forall i=1,2,\cdots,N$, in an n-dimensional Euclidean space.

Leader-following consensus is designed such that all the agents follow the trajectories of a virtual leader. In this case, the leader's dynamic is considered as follows:

$$\dot{\boldsymbol{p}}_r(t)=\boldsymbol{v}_r(t)\tag{2}$$

where $\boldsymbol{p}_r(t)$, $\boldsymbol{v}_r(t)\in\mathbb{R}^n$ are the position and velocity of the leader agent. The leader agent position can be manipulated through its velocity. Let us define the rigid desired-position formation from the agent i to its neighbors j, as $\boldsymbol{h}_i$, $\boldsymbol{h}_j\in\mathbb{R}^n$. According to [1], the classical leader-following formation control is given by

$$\boldsymbol{u}_i(t)=\sum_{j\in\mathcal{N}_i}a_{ij}[((\boldsymbol{p}_j(t)-\boldsymbol{p}_i(t))-(\boldsymbol{h}_j-\boldsymbol{h}_i))+(\boldsymbol{v}_j(t)-\boldsymbol{v}_i(t))]-(\boldsymbol{p}_i(t)-\boldsymbol{p}_r(t))-(\boldsymbol{v}_i(t)-\boldsymbol{v}_r(t))\tag{3}$$

where $\mathcal{N}_i$ is the set of i's neighbors.

Assumption 1 The graph $\mathcal{G}$ is an undirected graph.

Assumption 2 All the agents receive information states from the virtual leader agent.

Lemma 2 [24] The Laplacian matrix $\mathcal{L}$ associated with an undirected graph has at least one zero eigenvalue and all the nonzero eigenvalues are positive. The Laplacian matrix $\mathcal{L}$ has exactly one zero eigenvalue if and only if the graph is connected.

Using the consensus protocol (3), the MAS (1) achieves the desired formation if the following is satisfied:

$$\lim_{t\to\infty}\|(\boldsymbol{p}_i(t)-\boldsymbol{h}_i)-(\boldsymbol{p}_j(t)-\boldsymbol{h}_j)\|=0,\ \ \forall i=1,2,\cdots,N.\tag{4}$$

Bandwidth limitations, delays, or packet losses are challenges in real engineering applications in MASs. Let us define $\boldsymbol{\tau}_{ij}(t)$ as the communication faults between the agent i and the agent j. Based on $\boldsymbol{\tau}_{ij}(t)$, the leader-following formation control under communication faults (3) becomes

$$\boldsymbol{u}_i(t)=\sum_{j\in\mathcal{N}_i}a_{ij}[((\boldsymbol{p}_j(t-\tau_{ij}(t))-\boldsymbol{p}_i(t-\tau_{ij}(t)))-(\boldsymbol{h}_j-\boldsymbol{h}_i))+(\boldsymbol{v}_j(t-\tau_{ij}(t))-\boldsymbol{v}_i(t-\tau_{ij}(t)))]-(\boldsymbol{p}_i(t)-\boldsymbol{p}_r(t))-(\boldsymbol{v}_i(t)-\boldsymbol{v}_r(t)). \tag{5}$$

A degradation of the communication between agents can be associated to their distance as considered in [25]. Communication faults are considered dependent on the agent positions in link with the distance between them and described by the following function:

$$\tau_{ij}(t)=\left(\beta_1-\beta_1\mathrm{e}^{-\beta_2\boldsymbol{p}_i(t)-\boldsymbol{p}_j(t)}\right)(0.5-0.5\tanh(\beta_3(t-t_f))) \tag{6}$$

where β_1, β_2, and β_3 are positive constants, and t_f is the time of fault occurrence.

Assumption 3 The derivative of the communication fault $\dot{\tau}_{ij}(t)\leqslant d_\tau<1, \forall i\neq j, j\in\mathcal{N}_i$ where d_τ is a fixed scalar.

Note that, when $\tau_{ij}(t)=0$, the leader-following formation control problem can be solved using (3). Nevertheless, as reported in [24], the longest delay to reach the consensus is determined as $\tau_{ij}<\dfrac{\pi}{2\lambda_N(\mathcal{L})}$, where $\lambda_N(\mathcal{L})$ is the maximum eigenvalue of the Laplacian matrix, and the delay is considered constant with the same value for all agents in a fixed, undirected, and connected graph.

The problem under consideration in this paper is to design an event-triggered leader-following formation control such that all the agents follow the leader's trajectories subject to communication faults considered as smooth delays dependent on the agent positions.

3. Event-triggered leader-following formation control design

In the following subsections, a time-triggered formation control design and the event-triggered mechanism are presented in order to develop a strategy such that all the agents tolerate communication faults while reducing the information exchange.

3.1 Time-triggered leader-following formation control design

Let us define the error between the agent i and the leader as follows:

$$\begin{cases}\bar{\boldsymbol{p}}_i(t)=\boldsymbol{p}_i(t)-\boldsymbol{p}_r(t)\\ \bar{\boldsymbol{v}}_i(t)=\boldsymbol{v}_i(t)-\boldsymbol{v}_r(t)\end{cases}. \tag{7}$$

Let $\boldsymbol{\delta}_i(t)=\left[\bar{\boldsymbol{p}}_i(t)^{\mathrm{T}}-\boldsymbol{h}_i^{\mathrm{T}},\bar{\boldsymbol{v}}_i(t)^{\mathrm{T}}\right]^{\mathrm{T}}$, then the error dynamics can be rewritten as follows:

$$\begin{cases}\dot{\boldsymbol{\delta}}_i(t)=\boldsymbol{A}\boldsymbol{\delta}_i(t)+\boldsymbol{B}\boldsymbol{u}_i(t)\\ \boldsymbol{A}=\begin{bmatrix}0&I_n\\0&0\end{bmatrix}\\ \boldsymbol{B}=\begin{bmatrix}0\\I_n\end{bmatrix}\end{cases}. \tag{8}$$

Adding the control gain $\boldsymbol{K}_c\in\mathbb{R}^{n\times 2n}$ and the scalar α, the leader-following control (5) is modified in order to tolerate communication faults when $\tau_{ij}(t)>\dfrac{\pi}{2\lambda_N(\mathcal{L})}$ as follows:

$$\boldsymbol{u}_i(t)=\boldsymbol{K}_c\left[\sum_{j\in\mathcal{N}_i}a_{ij}(\boldsymbol{\delta}_i(t-\tau_{ij}(t))-\boldsymbol{\delta}_j(t-\tau_{ij}(t)))+\alpha\boldsymbol{\delta}_i(t)\right] \tag{9}$$

where $\boldsymbol{K}_c$ is the control gain to be designed and $\alpha>0$ must be a positive constant which represents the relationship between the leader and the followers. Based on (8), (7) becomes

$$\dot{\boldsymbol{\delta}}_i(t)=\boldsymbol{A}\boldsymbol{\delta}_i(t)+\boldsymbol{B}\boldsymbol{K}_c\Big[\sum_{j\in\mathcal{N}_i}a_{ij}(\boldsymbol{\delta}_i(t-\tau_{ij}(t))-\boldsymbol{\delta}_j(t-\tau_{ij}(t)))+\alpha\boldsymbol{\delta}_i(t)\Big]. \tag{10}$$

Let $\boldsymbol{\delta}(t)=[\boldsymbol{\delta}_1^{\mathrm{T}}(t),\boldsymbol{\delta}_2^{\mathrm{T}}(t),\cdots,\boldsymbol{\delta}_N^{\mathrm{T}}(t)]^{\mathrm{T}}$ and $\boldsymbol{\delta}(t-\tau)=[\boldsymbol{\delta}_1^{\mathrm{T}}(t-\tau_{1j}(t)),\boldsymbol{\delta}_2^{\mathrm{T}}(t-\tau_{2j}(t)),\cdots,\boldsymbol{\delta}_N^{\mathrm{T}}(t-\tau_{Nj}(t))]^{\mathrm{T}}$, then the error dynamics (9) are rewritten as follows:

$$\dot{\boldsymbol{\delta}}(t)=(\boldsymbol{I}_N\otimes(\boldsymbol{A}+\alpha\boldsymbol{B}\boldsymbol{K}_c))\boldsymbol{\delta}(t)+(\mathcal{L}\otimes\boldsymbol{B}\boldsymbol{K}_c)\boldsymbol{\delta}(t-\tau). \tag{11}$$

The following theorem provides LMI-based conditions for the computation of the control gain $\boldsymbol{K}_c$.

Theorem 1 Given the non-zero eigenvalues of the Laplacian matrix $\lambda_i(\mathcal{L}), i=2,3,\cdots,N$, scalars $\alpha>0$, $\mu_1>0$, $\mu_2>0$, and $\dot{\tau}_{ij}\leqslant d_\tau<1$, the leader-following consensus is quadratically stable under (9), if there exist symmetric matrices $\boldsymbol{P}_1>0$, $\boldsymbol{P}_2>0$, and a matrix $\boldsymbol{K}_c$ such that the following inequality

$$\begin{bmatrix}Q_1&0&Q_{2i}&Q_3\\ *&Q_4&-\mu_2\boldsymbol{K}_c^{\mathrm{T}}&0\\ *&*&-2\mu_2\boldsymbol{I}&0\\ *&*&*&-\boldsymbol{I}\end{bmatrix}<0 \tag{12}$$

holds $\forall i=2,3,\cdots,N$, with $Q_1=\mathrm{He}\{\boldsymbol{P}_1\boldsymbol{A}\}+\boldsymbol{I}-\dfrac{2\boldsymbol{P}_1}{\mu_1}+\boldsymbol{P}_2$, $Q_{2i}=-\lambda_i\boldsymbol{P}_1\boldsymbol{B}$, $Q_3=\dfrac{\boldsymbol{P}_1}{\mu_1}+\mu_1\alpha\boldsymbol{B}\boldsymbol{K}_c$, $Q_4=-(1-d_\tau)\boldsymbol{P}_2$.

Proof Let us define the following candidate Lyapunov functional inspired by [26]

$$\boldsymbol{V}=\boldsymbol{\delta}^{\mathrm{T}}(t)(\boldsymbol{I}_N\otimes\boldsymbol{P}_1)\boldsymbol{\delta}(t)+\int_{t-\tau}^{t}\boldsymbol{\delta}^{\mathrm{T}}(s)(\boldsymbol{I}_N\otimes\boldsymbol{P}_2)\boldsymbol{\delta}(s)\mathrm{d}s. \tag{13}$$

The time derivative of $\boldsymbol{V}$ along any solution of the system (11) is given by

$$\dot{\boldsymbol{V}} = 2\boldsymbol{\delta}^{\mathrm{T}}(t)(\boldsymbol{I}_N \otimes \boldsymbol{P}_1)\dot{\boldsymbol{\delta}}(t) + \boldsymbol{\delta}^{\mathrm{T}}(t)(\boldsymbol{I}_N \otimes \boldsymbol{P}_2)\boldsymbol{\delta}(t) - (1-\dot{\tau})\boldsymbol{\delta}^{\mathrm{T}}(t-\tau)(\boldsymbol{I}_N \otimes \boldsymbol{P}_2)\boldsymbol{\delta}(t-\tau). \quad (14)$$

According to [26] and Assumption 3, (14) is negative-definite when

$$\dot{\boldsymbol{V}} = 2\boldsymbol{\delta}^{\mathrm{T}}(t)(\boldsymbol{I}_N \otimes \boldsymbol{P}_1)\dot{\boldsymbol{\delta}}(t) + \boldsymbol{\delta}^{\mathrm{T}}(t)(\boldsymbol{I}_N \otimes \boldsymbol{P}_2)\boldsymbol{\delta}(t) - (1-d_\tau)\boldsymbol{\delta}^{\mathrm{T}}(t-\tau)(\boldsymbol{I}_N \otimes \boldsymbol{P}_2)\boldsymbol{\delta}(t-\tau) < 0, \quad (15)$$

thus,

$$\dot{\boldsymbol{V}} = 2\boldsymbol{\delta}^{\mathrm{T}}(t)(\boldsymbol{I}_N \otimes (\boldsymbol{P}_1(\boldsymbol{A} + \alpha\boldsymbol{P}_1\boldsymbol{B}\boldsymbol{K}_c)))\boldsymbol{\delta}(t) + 2\boldsymbol{\delta}^{\mathrm{T}}(t)(\mathcal{L} \otimes \boldsymbol{P}_1\boldsymbol{B}\boldsymbol{K}_c)\boldsymbol{\delta}(t-\tau) + \boldsymbol{\delta}^{\mathrm{T}}(t)(\boldsymbol{I}_N \otimes \boldsymbol{P}_2)\boldsymbol{\delta}(t) - (1-d_\tau)\boldsymbol{\delta}^{\mathrm{T}}(t-\tau)(\boldsymbol{I}_N \otimes \boldsymbol{P}_2)\boldsymbol{\delta}(t-\tau) < 0. \quad (16)$$

Let us perform a spectral decomposition of the Laplacian matrix $\mathcal{L}$, such that $\mathcal{L} = \boldsymbol{T}\boldsymbol{J}\boldsymbol{T}^{-1}$ with an invertible matrix $\boldsymbol{T} \in \mathbb{R}^{N\times N}$ and a diagonal matrix $\boldsymbol{J} = \mathrm{diag}(\lambda_1 = 0, \lambda_2, \cdots, \lambda_N)$. By Lemma 2, eigenvalues of $\mathcal{L}$ form a base of eigenvectors which are used to construct the invertible matrix $\boldsymbol{T}$. Let us define the following change of coordinates:

$$\begin{cases} \boldsymbol{\psi}(t) = (\boldsymbol{T}^{-1} \otimes \boldsymbol{I}_N)\boldsymbol{\delta}(t) \\ \boldsymbol{\psi}(t-\tau) = (\boldsymbol{T}^{-1} \otimes \boldsymbol{I}_N)\boldsymbol{\delta}(t-\tau) \end{cases}. \quad (17)$$

Taking (17) into (16) leads to

$$\dot{\boldsymbol{V}} = 2\boldsymbol{\psi}^{\mathrm{T}}(t)(\boldsymbol{I}_N \otimes (\boldsymbol{P}_1(\boldsymbol{A} + \alpha\boldsymbol{B}\boldsymbol{K}_c)))\boldsymbol{\psi}(t) + 2\boldsymbol{\psi}^{\mathrm{T}}(t)(\boldsymbol{J} \otimes \boldsymbol{P}_1\boldsymbol{B}\boldsymbol{K}_c)\boldsymbol{\psi}(t-\tau) + \boldsymbol{\psi}^{\mathrm{T}}(t)(\boldsymbol{I}_N \otimes \boldsymbol{P}_2)\boldsymbol{\psi}(t) - (1-d_\tau)\boldsymbol{\psi}^{\mathrm{T}}(t-\tau)(\boldsymbol{I}_N \otimes \boldsymbol{P}_2)\boldsymbol{\psi}(t-\tau). \quad (18)$$

By Lemma 2, it is obtained that $\boldsymbol{\psi}_1(t) = 0$ and $\boldsymbol{\psi}_1(t-\tau) = 0$ due to $\lambda_1 = 0$, then (18) is rewritten as follows:

$$\dot{\boldsymbol{V}} = \sum_{i=2}^{N} \boldsymbol{\psi}_i^{\mathrm{T}}(t)\mathrm{He}\{\boldsymbol{P}_1(\boldsymbol{A} + \alpha\boldsymbol{B}\boldsymbol{K}_c)\}\boldsymbol{\psi}_i(t) + 2\sum_{i=2}^{N} \boldsymbol{\psi}_i^{\mathrm{T}}(t)\lambda_i\boldsymbol{P}_1\boldsymbol{B}\boldsymbol{K}_c\boldsymbol{\psi}_i(t-\tau) + \sum_{i=2}^{N} \boldsymbol{\psi}_i^{\mathrm{T}}(t)\boldsymbol{P}_2\boldsymbol{\psi}_i(t) - (1-d_\tau)\sum_{i=2}^{N} \boldsymbol{\psi}_i^{\mathrm{T}}(t-\tau)\boldsymbol{P}_2\boldsymbol{\psi}_i(t-\tau). \quad (19)$$

Then, the following matrix is obtained:

$$\dot{\boldsymbol{V}} = \sum_{i=2}^{N} \begin{bmatrix} \boldsymbol{\psi}_i^{\mathrm{T}}(t) \\ \boldsymbol{\psi}_i^{\mathrm{T}}(t-\tau) \end{bmatrix}^{\mathrm{T}} \boldsymbol{\Omega}_i \begin{bmatrix} \boldsymbol{\psi}_i(t) \\ \boldsymbol{\psi}_i(t-\tau) \end{bmatrix} \quad (20)$$

where $\boldsymbol{\Omega}_i = \begin{bmatrix} \mathrm{He}\{\boldsymbol{P}_1(\boldsymbol{A} + \alpha\boldsymbol{B}\boldsymbol{K}_c)\} + \boldsymbol{P}_2 & \lambda_i\boldsymbol{P}_1\boldsymbol{B}\boldsymbol{K}_c \\ * & -(1-d_\tau)\boldsymbol{P}_2 \end{bmatrix}$.

If matrix $\boldsymbol{\Omega}_i < 0$, $\forall i = 2, 3, \cdots, N$, then $\dot{\boldsymbol{V}} < 0$; thus, the synchronization error between the leader and the followers is quadratically stable. Using Schur complement (Lemma 1) in (12), the following inequality is obtained:

$$\begin{bmatrix} \boldsymbol{R}_1 & 0 & Q_{2i} \\ * & Q_4 & -\mu_2\boldsymbol{K}_c^{\mathrm{T}} \\ * & * & -2\mu_2\boldsymbol{I} \end{bmatrix} < 0 \quad (21)$$

where $\boldsymbol{R}_1 = \mathrm{He}\{\boldsymbol{P}_1\boldsymbol{A}\} + \boldsymbol{I} - \dfrac{2\boldsymbol{P}_1}{\mu_1} + \boldsymbol{P}_2 + \left(\dfrac{\boldsymbol{P}_1}{\mu_1} + \mu_1\alpha\boldsymbol{B}\boldsymbol{K}_c\right)^{\mathrm{T}} \cdot \left(\dfrac{\boldsymbol{P}_1}{\mu_1} + \mu_1\alpha\boldsymbol{B}\boldsymbol{K}_c\right)$. The inequality (21) is pre- and post-multiplied by $\begin{bmatrix} \boldsymbol{I} & 0 & 0 \\ 0 & \boldsymbol{I} & -\boldsymbol{K}_c^{\mathrm{T}} \end{bmatrix}$ and its transpose, thus we obtain

$$\begin{bmatrix} \boldsymbol{R}_1 & Q_{2i} \\ * & Q_4 \end{bmatrix} < 0 \quad (22)$$

Note that:

$$\mathrm{He}\{\boldsymbol{P}_1(\boldsymbol{A} + \alpha\boldsymbol{B}\boldsymbol{K}_c)\} + \boldsymbol{P}_2 \leqslant \mathrm{He}\{\boldsymbol{P}_1(\boldsymbol{A} + \alpha\boldsymbol{B}\boldsymbol{K}_c)\} + \boldsymbol{P}_2 + \alpha^2(\boldsymbol{P}_1\boldsymbol{B}\boldsymbol{K}_c)^{\mathrm{T}}(\boldsymbol{P}_1\boldsymbol{B}\boldsymbol{K}_c) = \mathrm{He}\{\boldsymbol{P}_1\boldsymbol{A}\} + \boldsymbol{P}_2 - \frac{\boldsymbol{P}_1^2}{\mu_1^2} + \left(\frac{\boldsymbol{P}_1}{\mu_1} + \alpha\boldsymbol{B}\boldsymbol{K}_c\right)^{\mathrm{T}}\left(\frac{\boldsymbol{P}_1}{\mu_1} + \alpha\boldsymbol{B}\boldsymbol{K}_c\right) \quad (23)$$

where $\mu_1 > 0$. By taking into account the following inequality:

$$\begin{cases} \left(\boldsymbol{I} - \dfrac{\boldsymbol{P}_1}{\mu_1}\right)\left(\boldsymbol{I} - \dfrac{\boldsymbol{P}_1}{\mu_1}\right) \geqslant 0 \\ \boldsymbol{I} - \dfrac{2\boldsymbol{P}_1}{\mu_1} \geqslant -\dfrac{\boldsymbol{P}_1^2}{\mu_1^2} \end{cases} \quad (24)$$

and combining (23) and (24), the following is obtained:

$$\mathrm{He}\{\boldsymbol{P}_1(\boldsymbol{A} + \alpha\boldsymbol{P}\boldsymbol{B}\boldsymbol{K}_c)\} + \boldsymbol{P}_2 \leqslant \mathrm{He}\{\boldsymbol{P}_1\boldsymbol{A}\} + \boldsymbol{I} + \boldsymbol{P}_2 - \frac{2\boldsymbol{P}_1}{\mu_1} + \left(\frac{\boldsymbol{P}_1}{\mu_1} + \alpha\boldsymbol{B}\boldsymbol{K}_c\right)^{\mathrm{T}}\left(\frac{\boldsymbol{P}_1}{\mu_1} + \alpha\boldsymbol{B}\boldsymbol{K}_c\right). \quad (25)$$

Based on (25) and (22), $\boldsymbol{\Omega}_i < 0$ is recovered, thus, the LMI (12) corresponds to (20) and the synchronization error is quadratically stable under (9), thus completing the proof. □

Remark 1 Theorem 1 guarantees the time-triggered leader-following formation control design which is continuously updated.

3.2 Event-triggered mechanism

The following section, an event-triggered mechanism is developed in order to reduce the information exchange and the control update rate.

The update of the control law action in event-triggered approaches depends on an event error. This event error is calculated based on the last and the current state values. When the magnitude of the event error exceeds a threshold, the control law value is updated, otherwise, the control law keeps the last calculated value. The control in (9) is modified in order to design an event-triggered

mechanism as follows:

$$\boldsymbol{u}_i(t)=\boldsymbol{K}_c\Big[\sum_{j\in N_i}a_{ij}\Big(\boldsymbol{\delta}_i\Big(t_k^i-\tau_{ij}\Big(t_k^i\Big)\Big)-\boldsymbol{\delta}_j\Big(t_k^i-\tau_{ij}\Big(t_k^i\Big)\Big)\Big)+\alpha\boldsymbol{\delta}_i\Big(t_k^i\Big)\Big] \tag{26}$$

where $\boldsymbol{\delta}_i(t_k^i)$ and $\boldsymbol{\delta}_j(t_k^i)$ are the last values of the synchronization errors of agents i and j, respectively, and agent j; $\boldsymbol{\delta}_i(t_k^i-\tau_{ij}(t_k^i))$ and $\boldsymbol{\delta}_j(t_k^i-\tau_{ij}(t_k^i))$ are the last values of the delayed synchronization errors of agents i and j. The sequence of event-times $0\leqslant t_0^i\leqslant t_1^i\leqslant t_2^i\leqslant\cdots$ of the agent i is defined as $t_{k+1}^i=\inf\{t:t>t_k^i,f_i(\zeta_i(t))>0\}$. The agent i requests the information of the agent j at the event t_{k+1}^i in order to update the control law, otherwise, the control law keeps the last computed value. Let us define the event error as follows:

$$\begin{cases}\boldsymbol{\zeta}_i(t)=\boldsymbol{\delta}_i(t_k^i)-\boldsymbol{\delta}_i(t)\\ \boldsymbol{\zeta}_i(t-\tau_{ij}(t))=\boldsymbol{\delta}_i(t_k^i-\tau_{ij}(t_k^i))-\boldsymbol{\delta}_i(t-\tau_{ij}(t))\end{cases} \tag{27}$$

According to [7], if the leader-following consensus is quadratically stable, then, the following event function can be considered:

$$f_i(t)=\|\boldsymbol{\zeta}_i(t)\|-(c_1+c_2\mathrm{e}^{-c_3t}) \tag{28}$$

where parameters $c_1>0$, $c_2>0$, $0<c_3|\gamma_{\min}(\boldsymbol{A}+\alpha\boldsymbol{B}\boldsymbol{K}_c)|$, and $\gamma_{\min}(\boldsymbol{A}+\alpha\boldsymbol{B}\boldsymbol{K}_c)$ is the minimum eigenvalue of $(\boldsymbol{A}+\alpha\boldsymbol{B}\boldsymbol{K}_c)$.

4. Example: fleet of UAVs under communication faults

In order to illustrate the effectiveness of the proposed strategy, real implementations in a fleet of UAVs are presented in this section.

The experimental platform is described and some experimental results are shown in the following section. A video corresponding to the results can be found at https://youtu.be/Lo_kuGY9Wq4.

4.1 Experimental platform description

The experimental platform used for this implementation consists of an Optitrack system to recognize the UAVs in a three-dimensional space by image processing using Prime 17W cameras; Motive 2.1.1 is the software to manipulate the Optitrack which uses the virtual-reality peripheral network (VRPN) protocol with communication to a virtual machine; Ubuntu 16.04 is installed in the virtual machine with ROS Kinetic to manipulate the UAVs in parallel with Motive; identical Bebop 2 parrots are the UAVs (see Fig. 1). The code is developed in Python 2.7. The sample time is 0.02 s.

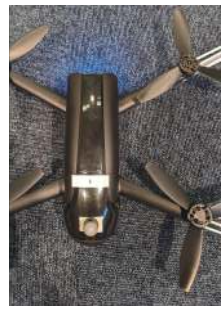

Fig. 1 Bebop 2 parrot

According to [27], a fleet of UAVs can be described as a second-order MAS if an inner closed-loop control is considered for each UAV employing their angles with the following references:

$$\begin{aligned}\psi_{d_i}(t)&=0,\\ \theta_{d_i}(t)&=\arctan\Big(\frac{u_{x_i}}{u_{z_i}+g}\Big),\\ \varphi_{d_i}(t)&=\arcsin\Bigg(-\frac{u_{y_i}}{\sqrt{u_{x_i}^2+u_{y_i}^2+(u_{z_i}+g)^2}}\Bigg),\\ T_i(t)&=m_{\mathrm{s}}\sqrt{u_{x_i}^2+u_{y_i}^2+(u_{z_i}+g)^2},\end{aligned} \tag{29}$$

where $\boldsymbol{u}_i(t)=[u_{x_i},u_{y_i},u_{z_i}]^{\mathrm{T}}$ is the consensus control law calculated using (5) (classical formation control $\boldsymbol{K}_c=\begin{bmatrix}-\boldsymbol{I} & -\boldsymbol{I}\end{bmatrix}$), (9) (time-triggered robust approach), and (27) (event-triggered approach); $\boldsymbol{\psi}_{d_i}(t)$, $\boldsymbol{\theta}_{d_i}(t)$, and $\boldsymbol{\varphi}_{d_i}(t)$ are the reference angles for each UAV; $m_{\mathrm{s}}=0.5$ kg is the mass of the UAV, which are considered to be homogeneous; $g=9.806\ \mathrm{m/s^2}$ is the acceleration of gravity.

The goal of the three UAVs is to form an isosceles triangle and follow the trajectories of a virtual agent with the following desired formation $\boldsymbol{h}_1=[0,0]^{\mathrm{T}}$, $\boldsymbol{h}_2=[0,1.5]^{\mathrm{T}}$, and $\boldsymbol{h}_3=[0.75,1.3]^{\mathrm{T}}$.

The LMI in Theorem 1 is solved with the following parameters: $\mu_1=1$, $\mu_2=10$, $\alpha=1$, and $d_\tau=0.2$ obtaining the control gain $\boldsymbol{K}_c=\begin{bmatrix}-(0.492\,2)\boldsymbol{I}_3 & -(0.976\,8)\boldsymbol{I}_3\end{bmatrix}$. This control gain is used in both the time-triggered and event-triggered approach. Table 1 shows the initial values of the UAVs.

Table 1 Initial conditions of the UAVs

Agent	Position $[x,y]$	Velocity
1	$[-0.724\,9,-0.723\,2]$	$[-0.008\,4,0.035\,7]$
2	$[0.033\,0,-0.334\,5]$	$[0.012\,9,-0.010\,7]$
3	$[1.511\,5,1.016\,7]$	$[-0.023\,9,0.008\,2]$

The communication topology is described by the following Laplacian matrix:

$$\mathcal{L}=\begin{bmatrix} 2 & -1 & -1 \\ -1 & 2 & -1 \\ -1 & -1 & 2 \end{bmatrix}. \tag{30}$$

The communication fault is implemented through an artificial function with the following parameters: $\beta_1 = 0.8$, $\beta_2 = 1$, $\beta_3 = 0.6$, and $t_f = 10$ s. All the UAVs are affected by the communication fault. The event-function has the following parameters: $c_1 = 0.03$, $c_2 = 3$, and $c_3 = 0.1$.

Three implementations have been carried out for comparing the performance of the classical formation control (5), the time-triggered robust approach (9), and the event-triggered approach (27). In the case of the classical formation control, the experiment had to be stopped to avoid the UAVs to crash.

4.2 Experimental results

Fig. 2 illustrates the obtained trajectories of the UAVs using the classical formation control. The UAVs should follow the trajectory of the virtual agent in black. However, due to the communication faults, they start to oscillate, and they cannot maintain the formation.

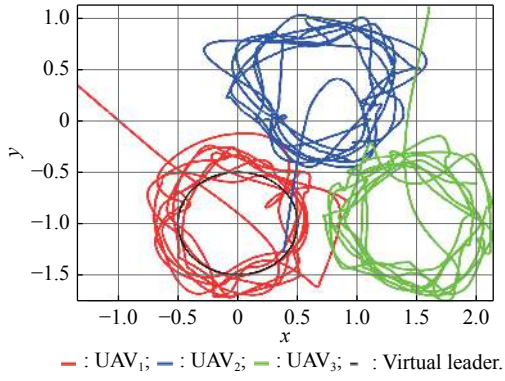

Fig. 2 Trajectories of UAVs (classical approach)

Fig. 3 shows the UAVs trajectories obtained using the time-triggered robust control. The UAVs present a decrease in the oscillations with respect to the previous case. Moreover, they maintain the desired formation.

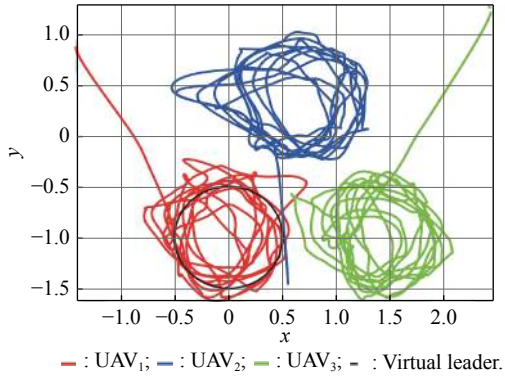

Fig. 3 Trajectories of UAVs (proposed time-triggered approach)

Fig. 4 presents the UAVs trajectories when the event-triggered mechanism is used. The UAVs present a better performance, maintaining the formation despite the communication faults.

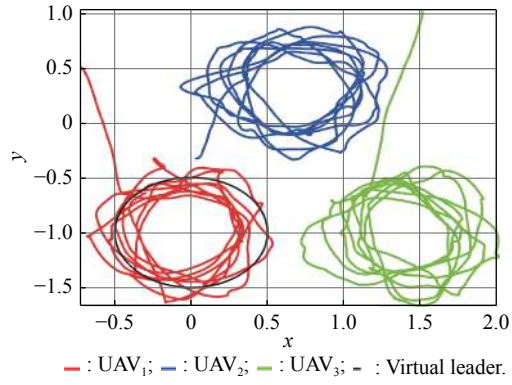

Fig. 4 Trajectories of UAVs (proposed event-triggered approach)

Fig. 5 presents the UAVs velocities obtained using the classical formation control. After approximately 140 s, the UAVs start to show stronger oscillations. As mentioned earlier, in order to preserve the integrity of the UAVs, the experiment has to be stopped.

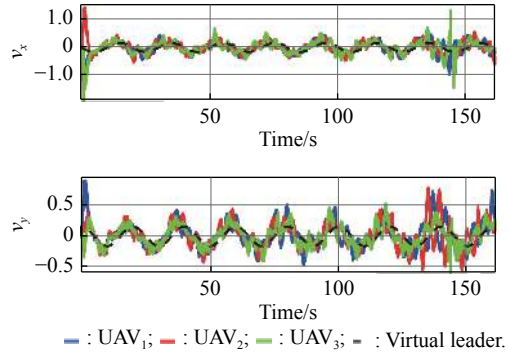

Fig. 5 Velocities of UAVs (classical approach)

Fig. 6 shows the UAVs ' velocities using the time-triggered robust control. The oscillations decrease when compared to the classical formation control. However, there is still a small offset between the leader velocities and the velocities of the UAVs. Also, an offset is observed, induced by the fact that the control gain is smaller than that in the classical formation control.

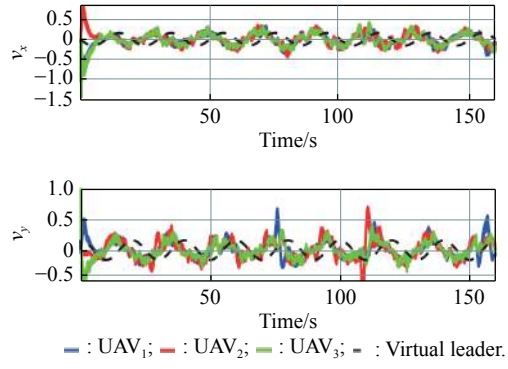

Fig. 6 Velocities of UAVs (proposed time-triggered approach)

Fig. 7 illustrates the UAVs' velocities using the event-triggered control. The oscillations are smaller compared to the other two approaches. However, the offset is still present due to the control gain. It is worth highlighting that the event-triggered control reduces the information exchange between the agents and the update rate of the control law.

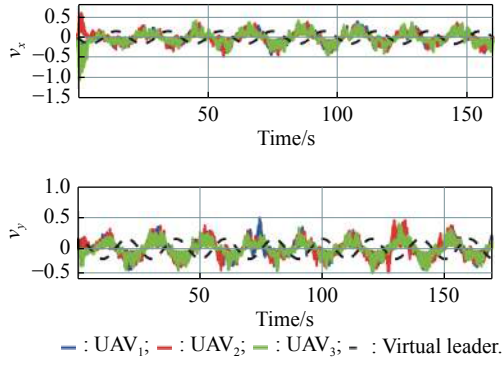

Fig. 7 Velocities of UAVs (proposed event-triggered approach)

Fig. 8 presents the event-triggered control law. The time interval between 15 s and 17 s is zoomed to illustrate when the control law keeps the last value.

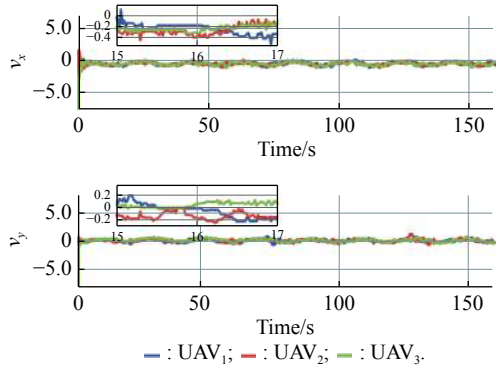

Fig. 8 Consensus control law (event-triggered proposed approach)

In order to measure the performance of the consensus, let us define $\boldsymbol{d}_{ij}=\bar{\boldsymbol{x}}_i-\bar{\boldsymbol{x}}_j$, where $\bar{\boldsymbol{x}}_i=[p_i-h_i \quad v_i]^{\mathrm{T}}$, and $\bar{\boldsymbol{x}}_j=[p_j-h_j \quad v_j]^{\mathrm{T}}$. Fig. 9 illustrates the evaluation of the performance of the consensus using the classical formation control. The performance presents oscillations after 140 s due to the communication faults.

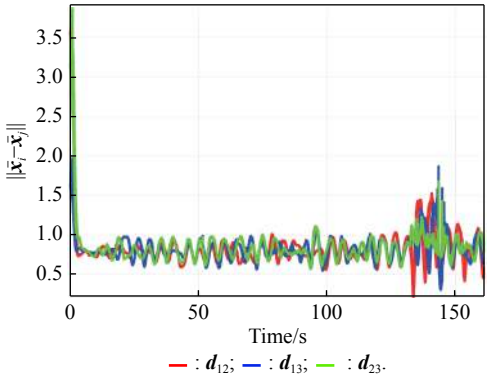

Fig. 9 Evaluation of consensus' performance (classical approach)

Fig. 10 shows the evaluation of the performance of the consensus using the time-triggered robust control. Compared to Fig. 9, the performance has been improved.

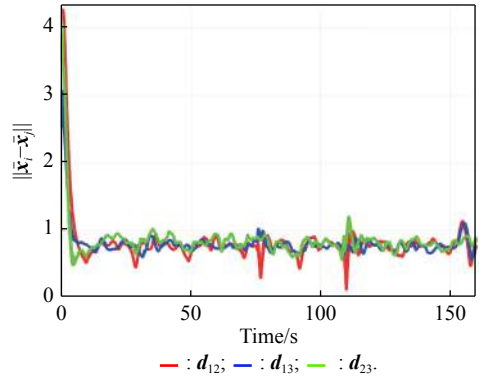

Fig. 10 Evaluation of the consensus' performance (proposed time-triggered approach)

Fig. 11 presents the evaluation of the consensus performance using the event-triggered control. Compared to Fig. 10, the performance is smaller than the threshold value 1 due to the desired formation.

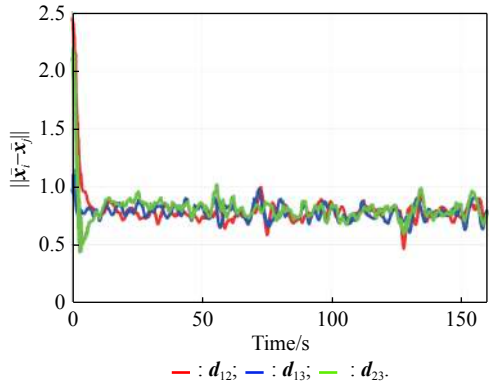

Fig. 11 Evaluation of consensus' performance (proposed event-triggered approach)

Fig. 12 presents the profile of the events for the event-triggered control. It is considered 1 for UAV$_1$, 2 for UAV$_2$, 3 for UAV$_3$ if an event occurs, respectively, and 0 if there is no event. A zoom is considered in some intervals in order to show when an event occurs.

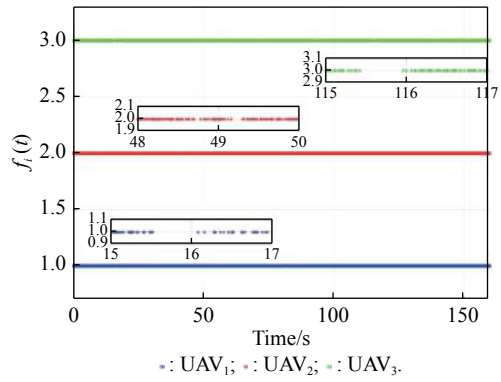

Fig. 12 Events for updating the control law

Fig. 13 shows the total number of events in each UAV. "No event" means that the control law and the exchange of information are not updated. For example, UAV_1 has 1 907 of no events compared with 6 556 events. In contrast with time-triggered, the update of the information and the control law has been reduced.

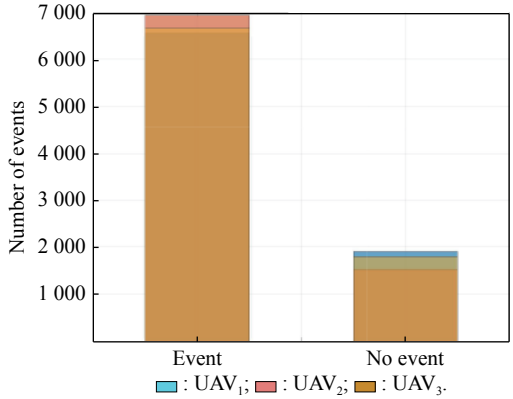

Fig. 13 Total number of events in each UAV

In order to quantify the performance between the approaches, the root mean square (RMS) metric is used. In Table 2, the RMS value of $\boldsymbol{d}_{ij}$ is presented for each combination of UAVs corresponding to the classical formation control, the time-triggered robust control, and the event-triggered control. It should be noted that the event-triggered approach reduces the energy consumption.

Table 2 Comparison of the consensus RMS

d_{ij}	Classical	Time-triggered	Event-triggered
d_{12}	0.9129	0.8947	0.8932
d_{13}	0.9060	0.8910	0.8818
d_{23}	0.9189	0.9088	0.8978

5. Conclusions

This paper has presented an event-triggered formation for second-order MAS under communication faults. The controller gain has been calculated by using LMI tools and an event-triggered mechanism has been introduced to reduce the information exchange between agents. The proposed approach has been implemented in a real platform of a fleet of UAVs subject to communication faults. A comparison between a state-of-the-art technique and the proposed technique has been provided, demonstrating the performance improvement brought by the proposed approach. For future work, a measurement of the energy consumption can be implemented in the real platform in order to compare the performance between the approaches.

References

[1] LI Z K, DUAN Z S. Cooperative control of multi-agent systems: a consensus region approach. London: CRC Press, 2014.

[2] NI W, CHENG D Z. Leader-following consensus of multi-agent systems under fixed and switching topologies. Systems & Control Letters, 2010, 59(3): 209–217.

[3] ZHANG Y Y, LI R F, ZHAO W, et al. Stochastic leader-following consensus of multi-agent systems with measurement noises and communication time-delays. Neurocomputing, 2018, 282: 136–145.

[4] CUI B, ZHAO C H, MA T D, et al. Leaderless and leader-following consensus of multi-agent chaotic systems with unknown time delays and switching topologies. Nonlinear Analysis: Hybrid Systems, 2017, 24: 115–131.

[5] JIANG J H, JIANG Y Y. Leader-following consensus of linear time-varying multi-agent systems under fixed and switching topologies. Automatica, 2020, 113: 108804.

[6] BELKADI A, CIARLETTA L, THEILLIOL D. Particle swarm optimization method for the control of a fleet of unmanned aerial vehicles. Journal of Physics: Conference Series, 2015, 659: 012015.

[7] VAZQUEZ TREJO J A, ROTONDO D, MEDINA M, et al. Observer-based event-triggered model reference control for multi-agent systems. Proc. of the International Conference on Unmanned Aircraft Systems, 2020: 421–428.

[8] DENG C, CHE W W, WU Z G. A dynamic periodic event-triggered approach to consensus of heterogeneous linear multiagent systems with time-varying communication delays. IEEE Trans. on Cybernetics, 2021, 51(4): 1812–1821.

[9] WANG Z D, YANG F W, HO D W C, et al. Robust H∞ control for networked systems with random packet losses. IEEE Trans. on Systems, Man, and Cybernetics, Part B (Cybernetics), 2007, 37(4): 916–924.

[10] CHEN C, XIE K, LEWIS F L, et al. Adaptive synchronization of multi-agent systems with resilience to communication link faults. Automatica, 2020, 111: 108636.

[11] LIU D, YANG G H. A dynamic event-triggered control approach to leader-following consensus for linear multiagent systems. IEEE Trans. on Systems, Man, and Cybernetics: Systems, 2020, 51(10): 6271–6279.

[12] LOSADA M G. Contributions to networked and event-triggered control of linear systems. Switzerland: Springer International Publishing, 2016.

[13] SEYBOTH G S, DIMAROGONAS D V, JOHANSSON K H. Event-based broadcasting for multi-agent average consensus. Automatica, 2013, 49(1): 245–252.

[14] LUNZE L. Control theory of digitally networked dynamic systems. Switzerland: Springer International Publishing, 2014.

[15] OBERMAISSER R. Event-triggered and time-triggered control paradigms. US: Springer, 2004.

[16] WANG Y L, CAO J D, WANG H J, et al. Event-triggering consensus for second-order leader-following multiagent systems with nonlinear time-delayed dynamics. International Journal of Control, Automation and Systems, 2020, 18(5): 1083–1093.

[17] REN J, QIANG S, GAO Y B, et al. Leader-following bipartite consensus of second-order time-delay nonlinear multi-agent systems with event-triggered pinning control under signed digraph. Neurocomputing, 2020, 385: 186–196.

[18] YE Y Y, SU H S. Leader-following consensus of general linear fractional-order multiagent systems with input delay via event-triggered control. International Journal of Robust and Nonlinear Control, 2018, 28(18): 5717–5729.

[19] TAN X, CAO J, LI X, et al. Leader-following mean square consensus of stochastic multi-agent systems with input delay via event-triggered control. IET Control Theory & Applications, 2017, 12(2): 299–309.

[20] CAI Y L, ZHANG H G, ZHANG J, et al. Distributed bipartite leader-following consensus of linear multi-agent systems with input time delay based on event-triggered transmission mechanism. ISA Transactions, 2020, 100: 221–234.

[21] VANZQUEZ TREJO J A, THEILLIOL D, MEDINA M, et

al. Leader-following formation control for networked multi-agent systems under communication faults/failures. Proc. of the Conference of Advances in Diagnostics of Processes and Systems, 2021, 313: 45−57.
[22] LANGVILLE A, STEWART W J. The Kronecker product and stochastic automata networks. Journal of Computational and Applied Mathematics, 2004, 167(2): 429–447.
[23] ZHOU K M, DOYLE J C. Essentials of robust control. New Jersey: Prentice Hall, 1998.
[24] OLFATI-SABER R, MURRAY R M. Consensus problems in networks of agents with switching topology and time-delays. IEEE Trans. on Automatic Control, 2004, 49(9): 1520–1533.
[25] GEORGES J P, THEILLIOL D, COCQUEMPOT V, et al. Fault tolerance in networked control systems under intermittent observations. International Journal of Applied Mathematics and Computer Science, 2011, 21(4): 639–648.
[26] KIM J H, PARK H B. H∞ state feedback control for generalized continuous/discrete time-delay system. Automatica, 1999, 35: 1443–1451.
[27] GUERRERO-CASTELLANOS J F, VEGA-ALONZO A, DURAND S, et al. Leader-following consensus and formation control of VTOL-UAVs with event-triggered communications. Sensors, 2019, 19(24): 5498.

Biographies

VAZQUEZ TREJO Juan Antonio was born in 1990. He received his B.S. degree in computer systems engineering at the Technological Institute of Zacatepec, Morelos, Mexico in 2013. He received his M.S. degree in automatic control at the National Research and Technological Development (CENIDET) in 2017. He obtained his Ph.D. degree in automatic control at CENIDET and the University of Lorraine in 2021. His current research interests include multi-agent systems and fault-tolerant control.
E-mail: juan-antonio.vazquez-trejo@univ-lorraine.fr

GUENARD Adrien was born in 1985. He is a research engineer at the Center for Automatic Control of Nancy (CRAN) with twelve years of experience in robotics and cyber-physical systems. He has been involved in many research projects with applications on mobile robots, UAVs, aeronautics, and control design. He is now in charge of the robotic platforms and manages an engineering team at Lorraine Research Laboratory in Computer Science and its Applications.
E-mail: adrien.guenard@loria.fr

ADAM-MEDINA Manuel was born in 1966. He received his professional diploma degree in electronic engineering of instrumentation from the Minatitlan Institute of Technology in 1991, his M.S. degree in electronics engineering from the CENIDET, Cuernavaca, Mexico, in 1995, and his Ph.D. degree in engineering from Henri Poincare University, Nancy, France, in 2004. He is currently a professor with the Department of Electronic Engineering, CENIDET. His current research interests are health aware control systems, model-based fault detection and isolation method synthesis and active fault tolerant control system design for linear parameter-independent, linear parameter-varying, and multi-linear systems.
E-mail: manuel.am@cenidet.tecnm.mx

PONSART Jean-Christophe was born in 1968. He received his Ph.D. degree in 1996 from the University of Savoie in Annecy, France, in nonlinear control of magnetic suspensions and its digital implementation aspects. In 1997, he participated in design and implementation of real time controllers with digital signal processor architecture for an industrial company. He has been with the Research Center for Automatic Control of Nancy (CRAN) at the University of Lorraine since 1998 as an assistant professor. He is currently a full professor from 2016 at the University of Lorraine. His current interests include fault diagnosis and accommodation, and fault-tolerant control applied to linear parameter varying and nonlinear systems and UAV applications among others.
E-mail: jean-christophe.ponsart@univ-lorraine.fr

CIARLETTA Laurent was born in 1974. He is an associate professor in information technology and computer science, the School of Mines of Nancy, Lorraine University. His current research interests include ambient computing, pervasive computing, and ubiquitous computing. The focus of his research is UAV and the Internet of Mobile and Smart Things.
E-mail: laurent.ciarletta@loria.fr

ROTONDO Damiano was born in 1987. He received his Ph.D. degree (with honors) from the Polytechnic University of Catalonia, Spain, in 2016. Since February 2020, he has been an associate professor at the Department of Electrical Engineering and Computer Science (IDE) of the University of Stavanger, in Norway. His main research interests include gain-scheduled control systems, fault detection and isolation and FTC of dynamic systems.
E-mail: damiano.rotondo@uis.no

THEILLIOL Didier was born in 1967. He is a research group co-leader at CRAN. He coordinates and leads national, European, and international R&D projects. He is currently an associate editor of ISA Transactions Journal, Journal of Intelligent and Robotic Systems and International Journal of Applied Mathematics & Computer Science. He was the General Chair and Program Chair of various international conferences sponsored by IEEE and IFAC. He is one of the steering committee members of European Advanced Control and Diagnosis and SysTol Association. His current research interests focus on health aware control framework based intelligent and classical model-based fault diagnosis method synthesis and active fault-tolerant control system design for linear time invariant, linear parameter varying, multi-linear systems, and reliability analysis.
E-mail: didier.theilliol@univ-lorraine.fr